Multifunctional Cyclic Phosphoramidate Solvent for Safe Lithium-Ion Batteries

Seongjae Ko[1], Ayaka Matsuoka[1], Wenting Chen[1], Taiga Iwata[1], Hiromi Otsuka[2], Shoji Yamaguchi[2], Takuya Masuda[2], Qifeng Zheng[1], Rui Shang[3,], Eiichi Nakamura[3], and Atsuo Yamada[1,4,*]*

1. Department of Chemical System Engineering, The University of Tokyo, 7-3-1 Hongo, Bunkyo-ku, Tokyo 113-8656, Japan

2. National Institute for Materials Science (NIMS), Tsukuba, Ibaraki 305-044, Japan

3. Department of Chemistry, The University of Tokyo, 7-3-1 Hongo, Bunkyo-ku, Tokyo 113-0033, Japan

4. SKKU Institute of Science & Technology (SIEST), Sungkyunkwan University, Suwon 16419, Korea

E-mail: rui@chem.s.u-tokyo.ac.jp
E-mail: yamada@chemsys.t.u-tokyo.ac.jp

Keywords: Li-ion batteries, non-flammable batteries, cyclic phosphoramidate, multifunctional solvents, safe electrolytes

Since the use of high-energy-density batteries continues to expand in large-scale applications, guaranteeing their safety is attracting increasing attention from the public sector and scientific communities. Considerable research efforts have been dedicated to identifying safer alternatives to the traditional electrolytes based on cyclic carbonate solvents, which represent the most flammable battery components. Nevertheless, developing functional electrolytes that may provide high safety and an uncompromised electrochemical performance remains challenging. In this study, a multifunctional non-flammable solvent with improved storage stability, viz. 2-(*N*,*N*-dimethylamino)-1,3,2-dioxaphospholane 2-oxide (DMAP), is synthesized. The DMAP-based electrolytes enable the formation of a stable passivation film with high electrochemical/thermal stabilities and the suppression of exothermic reactions, resulting in the high reversibility of graphite anodes along with improved battery safety. Strategic optimization of the molecular structures of cyclic phosphoramidates should be a promising approach towards preparing highly safe batteries with high energy densities.

TOC GRAPHICS

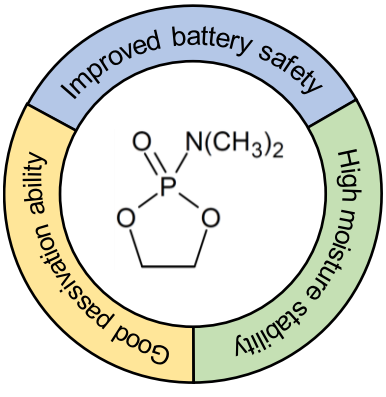

Li-ion batteries are widely utilized as energy storage devices in portable electronics and electric vehicles due to their high energy densities.[1–3] However, the increasing demand for large-scale batteries raises significant safety concerns.[4,5] Exothermic reactions induced by the thermal/chemical instabilities of the electrolyte solvent and the reduction products of the electrolyte (i.e., the solid electrolyte interphase (SEI)), in particular, are major factors contributing to fires and explosions.[6–9]

The redox potential of the graphite anode (0.1 V vs. Li/Li^+) in a Li-ion battery is located outside the thermodynamic potential windows of most electrolytes (typically 0.6–4.3 V vs. Li/Li^+), resulting in continuous electrolyte reduction at the graphite surface.[10,11] To address this problem, the cyclic carbonate solvent ethylene carbonate (EC) has been introduced as an electrolyte solvent.[10,11] EC aids in forming a stable SEI, which kinetically hinders electrolyte decomposition on the surface of the graphite anode by preventing direct contact between the electrolyte and electrode. However, the EC-derived SEI generally reacts easily with strongly Lewis-acidic PF_5 and Brønsted-acidic HF, which are generated via the thermal and/or chemical decomposition of the electrolyte salt $LiPF_6$.[7–9,12,13] This exothermic reaction at ≤150 °C is an early-stage initiator of sequential heat generation and thermal runaway in batteries.[7,9,13] By using an alternative salt, such as LiFSI ($LiN(SO_2F)_2$), the heat generation from SEI decomposition could be mitigated. However, direct exothermic reactions between a lithiated graphite anode and LiFSI salt at ≥150°C are known to be substantially significant than those with $LiPF_6$ salt.[14] Additionally, the high flammability of EC further exacerbates the vulnerabilities of batteries to ignition and explosion.[6]

Over the past decades, significant research effort has been dedicated to exploring electrolyte solvents that ensure high safety without compromising the electrochemical performances of batteries, e.g., linear P-based solvents, such as trimethyl phosphite and trimethyl phosphate,

were studied due to their non-flammability and exceptional capacities to scavenge radicals, Lewis acids, and HF, thereby mitigating the exothermic reactions of batteries.[15,16] However, most linear P-based solvents may not form a stable SEI on the graphite anode, inevitably leading to a poor cycling performance, with severe exfoliation of the graphene layers.[17–20] As another alternative, fluorinated solvents, such as fluorinated acetates and ethers, were developed.[21,22] These fluorinated solvents exhibit promising electrochemical properties, such as the ability to form a functional SEI, a high oxidation tolerance, and non-flammability. However, significant drawbacks, including high volatilities, limited scavenging capacities, and complex, toxic synthesis processes, hinder their practical utilization in commercial battery applications.

Recently, a cyclic phosphoramidate-based solvent, viz. 2-(2,2,2-trifluoroethoxy)-1,3,2-dioxaphospholane 2-oxide (TFEP), was synthesized to combine the chemical structures of a cyclic carbonate, with an SEI-forming capacity, and a non-flammable-phosphate group.[23] The TFEP-based electrolyte displays high stability towards the graphite anode and provides a high level of safety for batteries. However, its utilization has only been evaluated with a high-cost imide salt. Additionally, most cyclic phosphates are susceptible to ring-opening oligomerization due to nucleophilic attack at the P atom by residual H_2O in the electrolyte, thus requiring a highly moisture-controlled environment for storage.[24,25]

Herein, we report a strategically designed cyclic phosphoroamidate solvent, 2-(*N*,*N*-dimethylamino)-1,3,2-dioxaphospholane-2-oxide (DMAP), wherein an amino group with a low electronegativity is introduced adjacent to the P atom to mitigate the moisture sensitivity. DMAP-based electrolytes were investigated using different types of Li salts (LiFSI or $LiPF_6$) and linear carbonates (2,2,2-trifluoroethyl methyl carbonate (FEMC) or dimethyl carbonate (DMC)). The details of the design rationale of the solvent, its electrochemical compatibilities

with graphite anodes and $LiFePO_4$ cathodes, and the contributions of the DMAP-based electrolytes to battery thermal safety are demonstrated in the following sections.

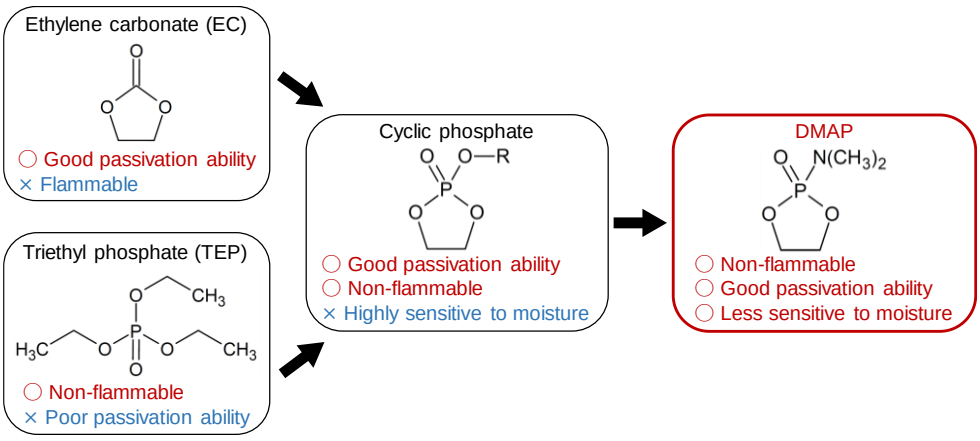

Figure 1. Design rationale of the cyclic phosphoramidate-based solvent DMAP. The five-membered cyclic phosphoramidate solvent DMAP was synthesized to harness the advantages of cyclic carbonates (SEI formation) and P-based solvents (non-flammability and radicals-/high Lewis acid-/HF-scavenging capacities). To mitigate the moisture sensitivity of the solvent, one O atom in the cyclic phosphate was substituted with a N atom of lower electronegativity, thus suppressing nucleophilic attack at the P atom caused by H_2O contamination of the electrolyte.

DMAP, which is a five-membered ring cyclic phosphoramidate with an *N*, *N*-dimethyl amino moiety, was synthesized as a multifunctional solvent (**Figures 1** and **S1**). By combining the molecular structures of traditional cyclic carbonates (e.g., EC) and linear P-based solvents (e.g., triethyl phosphate), unique functionalities, such as stable SEI formation and non-flammability (**Figure S2**), are realized.[23] Additionally, the high capacities for scavenging radicals, Lewis acids, and HF, which are due to the lone-pair-rich P and O atoms and Lewis-base P–N bond in the molecule, improve battery safety, with suppressed exothermic reactions at the anode.[16,26]

The N atom exhibits lower electronegativity than an O atom. Thus, the substitution of an O atom with a N atom mitigates the ring-opening reaction (oligomerization) by reducing the nucleophilic attack at the P atom caused by H_2O contamination of the electrolyte, as confirmed using ^{31}P-NMR spectroscopy (**Figure S3**). The peak representing the cyclic phosphoramidate

is exclusively observed, even after storage for one week with 10000 ppm of H_2O, confirming the high moisture stability of DMAP.

The passivating ability and safety contribution of DMAP were evaluated using model electrolytes, either with DMAP as a co-solvent (1 mol L^{-1} (M) LiFSI or $LiPF_6$/DMAP:linear carbonates (FEMC or DMC)), or as an electrolyte additive in the commercial electrolyte (1 M $LiPF_6$/EC:DMC + 1 wt% DMAP). The linear carbonates were mixed with DMAP to reduce the electrolyte viscosity.

The use of highly safe P-based solvents as battery electrolytes has been limited due to their poor SEI-forming capacities, leading to the exfoliation of graphite anodes and continuous electrolyte reduction.[17–20] Due to the cyclic structure similar to that of EC[10,11], the SEI comprising decomposition products of DMAP enables the high reversibility of graphite anodes, as shown in **Figure 2**. For instance, the graphite|Li coin half-cells containing electrolytes without DMAP, 1 M LiFSI/FEMC and 1 M $LiPF_6$/FEMC, exhibit severe electrolyte decomposition with large irreversible capacities during charging (lithiation) (23% and 31% of the initial Coulombic efficiency, respectively), suggesting the absence of stable SEIs on the graphite surfaces (**Figures 2a** and **2b**).

Conversely, largely improved initial Coulombic efficiencies (80% and 75%, respectively) and negligible capacity decay is observed in the DMAP-based electrolytes, 1 M LiFSI/DMAP:FEMC and 1 M $LiPF_6$/DMAP:FEMC, with high average Coulombic efficiencies of 99.99% (from the 10^{th} to the 300^{th} cycle) over 300 cycles at a slow current of 0.5C (**Figures 2c–2e, and S4-S7**). Therefore, the graphite surfaces are completely protected by the stable DMAP-derived SEIs, minimizing the reductive decomposition of the electrolytes.

To better understand the favorable effect of DMAP on SEI formation, X-ray photoelectron spectroscopy (XPS) of the graphite anodes was performed before and after cycling in the DMAP-based electrolytes (**Figures 3a, S7,** and **S8**). The intensities of the peaks representing the C–C bonds of graphite in the spectra of the cycled electrodes are drastically reduced, indicating that the graphite surfaces are covered by electrolyte-derived components. Furthermore, the detection of Li–P–O, Li–O, and Li–N in the Li 1s, P 2p, N 1s, and O 1s spectra confirms the formation of Li^+-conducting functional SEIs[27,28], which is attributed to the reduction of DMAP (i.e., DMAP + Li^+ + e^- → Li_2O + $LiPO_x$ + Li_3N + polyphosphate + *etc*., **Figures 3, S7, and S8**). This is consistent with our previous study[23], in that the reduction of the cyclic phosphate contributes to the formation of a functional SEI on the anode. The transmission electron microscopy (TEM) observation and energy dispersive X-ray spectroscopy (EDS) analysis also proved the presence of a few nanometer-scale thin DMAP-derived SEI layer on the graphite anode (**Figures S9 and S10**). Notably, SEI formation involves the simultaneous reduction of the Li salt, which provides functional SEI species, such as LiF (**Figures S7** and **S8**). However, salt-derived SEI components are not critical for the high reversibility of the graphite electrode, because DMAP-based electrolytes offer high cycle stabilities, regardless of the type of Li salts (LiFSI or $LiPF_6$), as shown in **Figure 2**. Therefore, the reduction of DMAP is crucial in the formation of the stable SEI, rather than that of the Li salt.

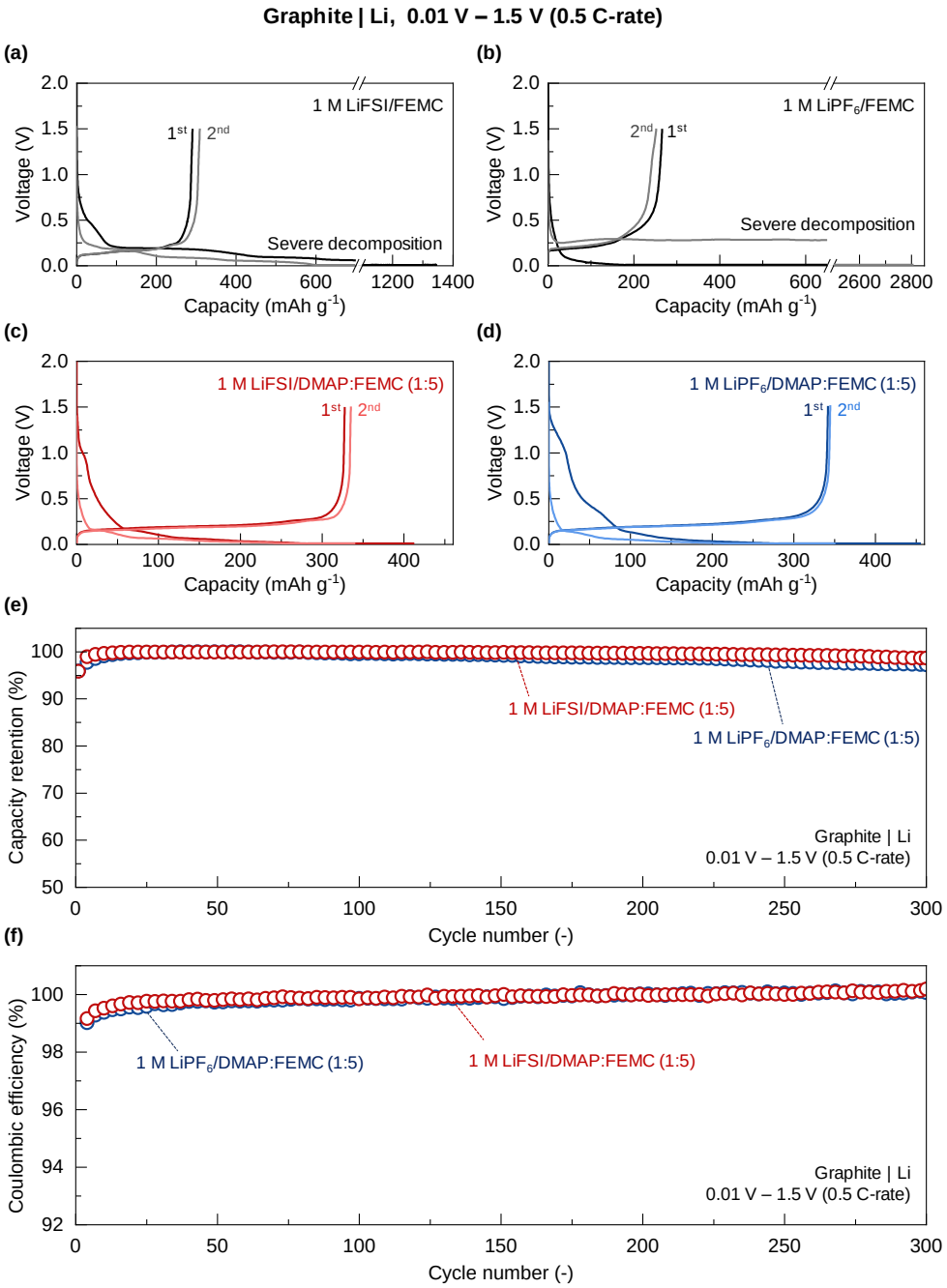

Figure 2. Highly reversible graphite anodes in DMAP-based electrolytes. The charge (lithiation)/discharge (delithiation) curves of graphite|Li coin half-cells in (a) 1 M LiFSI/FEMC, (b) 1 M $LiPF_6$/FEMC, (c) 1 M LiFSI/DMAP:FEMC, and (d) 1 M $LiPF_6$/DMAP:FEMC electrolytes. (e) Long-term cycling stabilities and (f) Coulombic efficiencies of cells containing the given electrolytes. The introduction of DMAP ensures the high reversibility of the graphite anodes. The results obtained with a different molar ratio of DMAP and FEMC are shown in **Figure S4**.

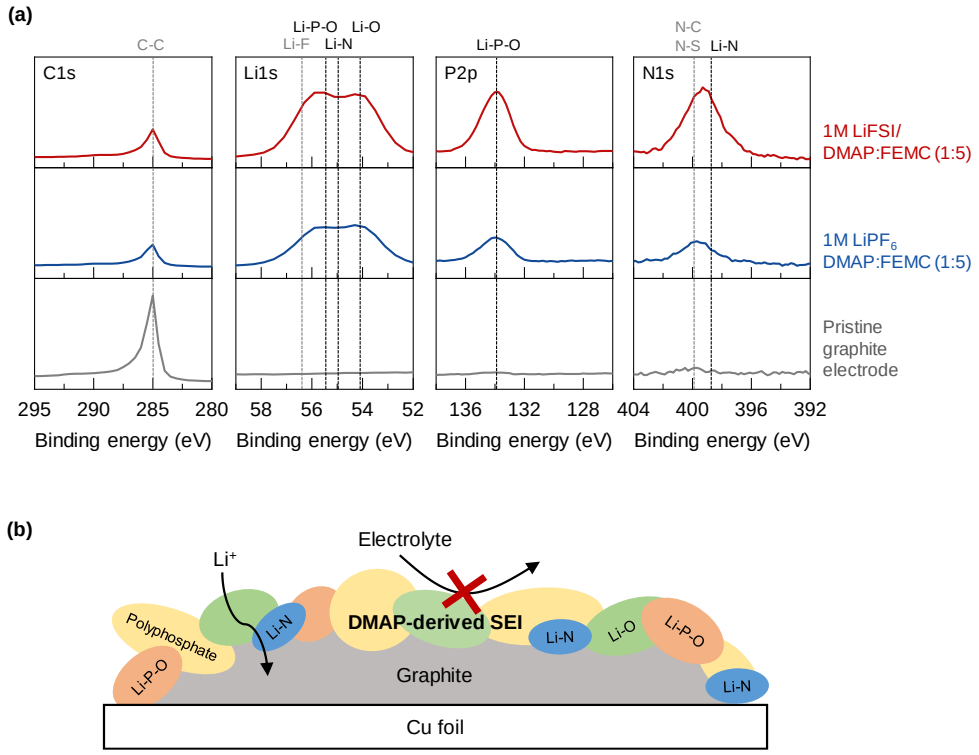

Figure 3. DMAP-derived SEI. (a) C 1s, Li 1s, P 2p, and N 1s XPS spectra of the pristine graphite electrode and those cycled in the given electrolytes. Peaks representing the Li–P–O, Li–O, and Li–N bonds are observed in the Li 1s, P 2p, and N 1s spectra of the samples cycled in the DMAP-based electrolytes, indicating the formation of DMAP-derived Li^+-conducting functional SEIs.[26–28] (b) Schematic of the DMAP-derived SEI formed on the graphite surface, which aids in suppressing electrolyte decomposition.

After confirming that the DMAP-derived SEI effectively prevents the reductive decomposition of the electrolyte, we also evaluated its contribution to battery safety via differential scanning calorimetry (DSC). **Figure 4** shows the DSC thermograms of fully lithiated graphite in the given electrolytes, measured in a tightly sealed container under Ar. A distinct decrease in heat generation associated with SEI thermal decomposition (≤150 °C) and direct lithiated graphite (C_xLi, x≥6)/electrolyte reactions (≥150 °C) are observed upon cycling in the DMAP-based electrolytes.[9,12,13] Notably, the pure FEMC electrolyte was excluded from this study because it displays a poor SEI-forming capacity, and thus, fully lithiated graphite did not form (**Figures 2a** and **2b**).

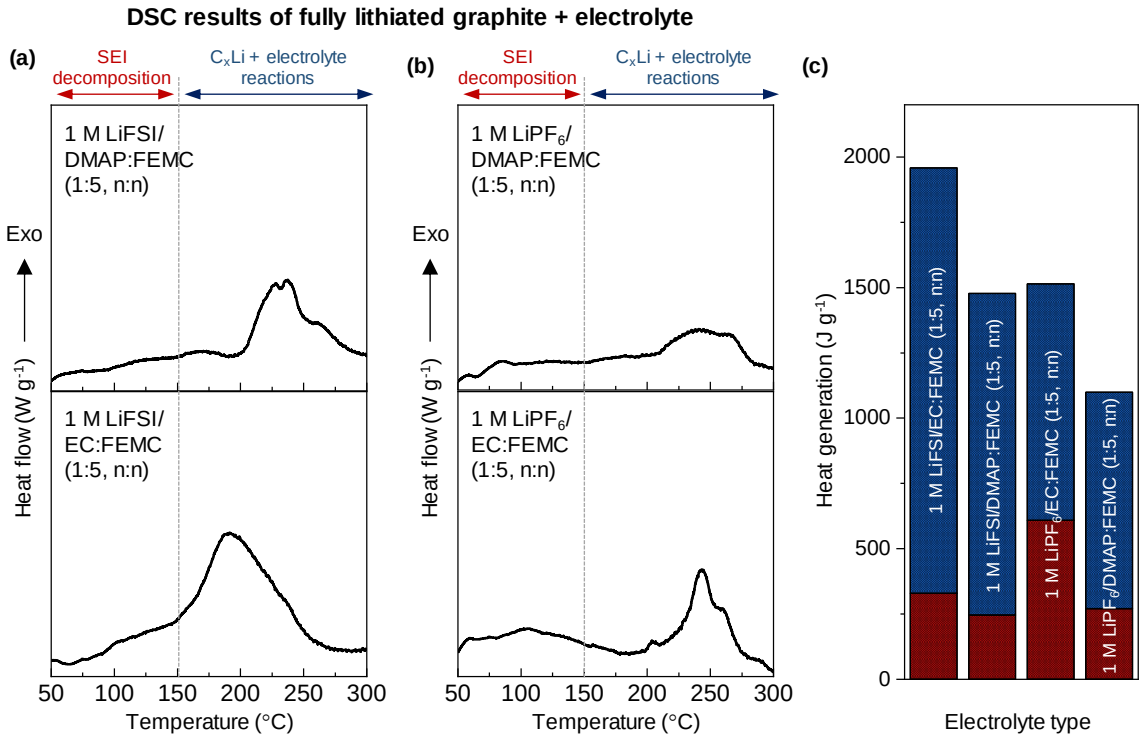

Figure 4. Enhanced thermal stabilities of the anodes in DMAP-based electrolytes. DSC thermograms and overall heat generation of fully lithiated graphite in the given electrolytes. A tightly sealed container with an Ar atmosphere, 25 mg of fully lithiated graphite powder, and 15 mg of electrolyte was heated to 200 °C at 0.5 °C min^{-1}. The unique properties of DMAP and the DMAP-derived SEI, such as high radicals-, Lewis acid-, and HF-scavenging capacities, contribute to improving the thermal stabilities of the anodes.

The effects of the salt and solvent on the thermal stability of a battery have been extensively investigated[9,12,13], e.g., $LiPF_6$ is chemically/thermally unstable, and it decomposes easily into strongly Lewis-acidic PF_5 and Brønsted-acidic HF, which further attack EC-derived organic compounds, such as alkyl carbonates, in the SEI.[7,9,13] On the other hand, LiFSI reacts directly with lithiated graphite (C_xLi, $x \geq 6$) at ≥150 °C, producing considerable heat.[14] These SEI thermal decompositions and reactions between the electrolyte (salt) and lithiated graphite increase overall heat generation and initiate thermal runaway.[7,9,13] Against these severe exothermic reaction, DMAP exhibits high scavenging capacities for radicals, Lewis acids, and HF, which are attributed to the presence of lone-pair-rich P and O atoms and the highly Lewis basic P–N bond in its molecular structure.[16,26] Furthermore, DMAP-derived SEI components, such as $LiPO_x$ and polyphosphate (**Figures 3 and S7-S10**), display high thermal and chemical

stabilities[29–32] and effectively scavenge Lewis acids[16], thus contributing further to the mitigation of the exothermic reactions. DMAP improves the reduction and thermal stabilities of anodes, regardless of the type of Li salts (LiFSI or $LiPF_6$) and co-solvents (FEMC or DMC) used, via its inherently high radicals-/Lewis acid-/HF-scavenging capacities and by forming an electrochemically/chemically/thermally stable SEI on the graphite surface (**Figures S11 and S12**). All the unique properties of DMAP are evident, regardless of whether it is used as an electrolyte co-solvent or additive (**Figures 2-4 and S11-S15**).

In this study, an O group was substituted with an amino functional group in the cyclic phosphate to reduce the excessive moisture sensitivity of the solvent (**Figures 1** and **S3**). However, N is less electronegative than O, which could increase the level of the highest occupied molecular orbital (HOMO), thus decreasing the thermodynamic oxidation stability of the electrolyte.[33–35] To evaluate the anodic limits of the electrolytes, linear sweep voltammetry (LSV) was performed using a Pt|Li|Li three-electrode cell. The anodic current begins to flow at ≤4.0 V vs. Li/Li^+ in DMAP-based electrolytes, which is slightly lower than that observed in electrolytes without DMAP (4.3 V vs. Li/Li^+, **Figure S16**). The oxidation stability of DMAP-based electrolytes is not sufficient for layered oxide cathodes such as $LiCoO_2$ and $LiNi_xCo_yMn_zO_2$. However, it is suitable for the $LiFePO_4$ cathode, which is widely used in electric vehicle batteries due to the reasonable redox potential of the abundant Fe^{2+}/Fe^{3+} redox couple (≤3.7 V vs. Li/Li^+), high theoretical capacity (170 mAh g^{-1}), and thermal stability (slow O_2 release at ≥700 °C).[36,37] As shown in **Figures 5 and S17-S19,** the use of DMAP as an electrolyte co-solvent or additive results in the highly stable operation of the $LiFePO_4$ electrode. For instance, the DMAP-based electrolytes, retain >93% of the discharge capacities of $LiFePO_4$|Li coin half-cells after 300 cycles at a slow current of 0.1C (equivalent to 8 months of evaluation).

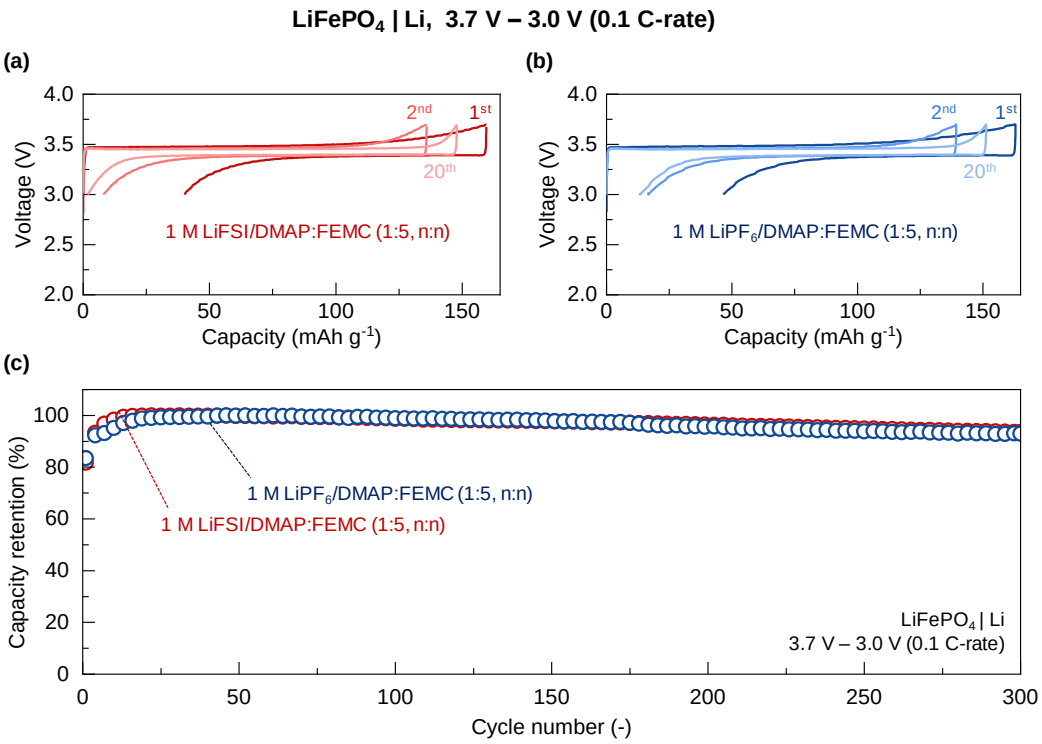

Figure 5. Electrochemical performances of $LiFePO_4$ cathodes in DMAP-based electrolytes. (a–b) Charge (delithiation)/discharge (lithiation) curves and (c) long-term (> 8 months) cycling stabilities of $LiFePO_4$|Li coin half-cells in 1 M LiFSI/DMAP:FEMC and 1 M $LiPF_6$/DMAP:FEMC electrolytes at a slow 0.1 C-rate. The increase in capacity during the initial cycles may be attributed to the activation of the cell via complex interactions between the cathode, anode, binder, and electrolyte.[38,39]

Moreover, DMAP helps to retard oxidative dissolution of the Al cathode current collector. **Figure S20** illustrates the results of the Al|Li floating test with various electrolytes. In 1 M LiFSI/FEMC:DMAP (1:5, n:n), the leakage current commenced at around 5.4 V, which is substantially higher than in 1 M LiFSI/FEMC (4.6 V). The XPS results of the Al surface before and after the floating test demonstrate that the peak intensity of P elements (Li-P-O and polyphosphate) increases between 4.5 and 5.0 V, while the peaks attributed to Al and Al_2O_3 are greatly reduced. This indicates that Al passivation is electrochemically induced by the sacrificial oxidation of the DMAP solvent.

However, the lab-synthesized DMAP contains a high level of H_2O contamination (78 ppm), which is one order of magnitude higher than that of the commercial 1 M $LiPF_6$/EC:DMC (1:1, v:v) electrolyte (≤8 ppm). The H_2O contamination may accelerate the hydrolysis/decomposition of the Li salt and solvent at the cathode surface[40] and the dissolution of transition metals in the cathode material[40,41], which may lead to a poor Coulombic efficiency (**Figure S18**). Also, there is a possibility that the lab-synthesized DMAP solvent may contain a small amount of impurities, which cannot be detected by NMR, yet could lead to side reactions with cell components such as electrodes, carbons, and coin cell cases. Thus, the $LiFePO_4$|graphite coin full-cells was not demonstrated. Overall, $LiFePO_4$ cathodes are highly reversible in DMAP-based electrolytes, although further purification and optimization of the electrolyte is required to decrease the side reactions.

The multifunctional solvent DMAP was synthesized by incorporating an amine moiety into a five-membered cyclic phosphate. The distinct molecular structure of DMAP, with an amino group, provides three key advantages: (i) significant suppression of reductive electrolyte decomposition by forming a stable DMAP-derived SEI, enabling the high reversibility of graphite anodes (>97% capacity retention after 300 cycles, with an average Coulombic efficiency of 99.99%, at a slow current of 0.5C), (ii) effective scavenging of radicals, Lewis acids, and HF, improving battery safety via a drastic reduction in the heat generated by the anode, (iii) considerably improved moisture sensitivity, with suppressed ring-opening oligomerization, yielding an enhanced storage stability. The DMAP-based electrolytes display moderate oxidation stabilities (≤4.0 V vs. Li/Li^+) due to their higher HOMO levels, yet these stabilities are sufficient to realize the stable cycling of $LiFePO_4$ cathodes. Importantly, all these chemical, electrochemical and thermal advantages can be obtained with electrolytes using DMAP as both a solvent and an additive, regardless of the type of salts (LiFSI or $LiPF_6$) and co-solvents (FEMC or DMC) used. Molecular modification, coupled with the fine-tuning of the elements in the molecular structure, may enable the optimization of the physicochemical and electrochemical properties, thereby opening up novel possibilities for extremely safe batteries with high energy densities.

Synthesis of DMAP: Dimethylamine (2.0 mol L^{-1} in tetrahydrofuran (THF), 32.8 g, 77 mmol, Sigma Aldrich, St. Louis, MO, USA) was added to anhydrous THF (80 mL, Fujifilm Wako Pure Chemical, Osaka, Japan) in a flask in an ice-water bath. A mixture of 2-chloro-1,3,2-dioxaphospholane 2-oxide (5 g, 35 mmol, Sigma Aldrich) and anhydrous THF (20 mL) was then added slowly to the dimethylamine/THF mixture with stirring, and the resultant mixture was stirred overnight. After completion of the reaction, the remaining dimethylamine hydrochloride and THF were respectively removed via filtration and rotary evaporation (80 mbar at 45 ℃). The obtained product was added to diethyl ether (100 mL, Fujifilm Wako Pure Chemical). Finally, the DMAP-containing ether layer was separated from the oil-state by-products, and the ether was evaporated at 50 °C and a pressure of 40 mbar. As a further purification process, the obtained DMAP was vacuum dried at room temperature in a glass tube for several days.

Characterization of DMAP: NMR spectroscopy was conducted to verify the formation of the target compound. The spectra, which confirmed the successful synthesis of DMAP, were recorded at room temperature using ^{1}H-NMR (500 MHz), ^{13}C-NMR (125 MHz), and ^{31}P-NMR (202 MHz) spectroscopy. ^{1}H NMR ($CDCl_3$, ppm): δ 4.15–4.24 (OCH_2CH_2O), 2.8 (6H); ^{13}C NMR ($CDCl_3$, ppm): δ 66.5 (OCH_2CH_2O), 36.5 (CH_3). The moisture stability of DMAP was evaluated via ^{31}P NMR spectroscopy (calibrated using H_3PO_4, ppm). The detailed spectra are shown in **Figures S1 and S3**.

Electrolyte preparation: The Li salt (LiFSI, Nippon Shokubai, Tokyo, Japan or $LiPF_6$, Kishida Chemical, Osaka, Japan) was mixed with mixtures of solvents (DMAP:FEMC (Halocarbon Products, Peachtree Corners, GA, USA), DMAP:DMC (Kishida Chemical, Osaka, Japan)) in an Ar-filled glovebox. The commercial electrolyte, 1 M $LiPF_6$/EC:DMC (1:1, v/v), was purchased from Kishida Chemical.

Electrode preparation: The electrodes used in this study were prepared as follows: a mixture of graphite powder (SNO10, SEC Carbon, Amagasaki, Japan) and carboxymethylcellulose binder (CMC, Daicel, Osaka, Japan) in a mass ratio of 96:4 was prepared to fabricate the graphite electrode. A mixture of $LiFePO_4$ powder (BTR New Material Group, Shenzhen, China), acetylene black (Li400, Denka Black, Denka, Tokyo, Japan), and CMC in a mass ratio of 86:10:4 was prepared to fabricate the $LiFePO_4$ electrode. Cu (Fchikawa Rare Metal, Tokyo, Japan) and Al (Fchikawa Rare Metal, Tokyo, Japan) foils were used as the anode and cathode current collectors, respectively. The prepared electrodes were vacuum dried at 120 °C for >3 h and then stored in an Ar-filled glovebox prior to use. The loading levels of the graphite and $LiFePO_4$ electrodes were approximately 2 mg cm^{-2}.

Electrochemical measurements: All electrochemical measurements were performed at room temperature. The coin half-cells were assembled in an Ar-filled glovebox using 2032-type cell components (cathode and anode cans, gasket, wave washer, and spacer) purchased from Hohsen, Osaka, Japan. A graphite or $LiFePO_4$ electrode was used as the positive electrode, and Li metal (Honjo Chemical, Neyagawa, Japan) was used as the negative electrode. An adequate amount of electrolyte (80 µL) was applied to fully soak the electrode and glass fiber-type separator (GC50, Advantec, Tokyo, Japan). The coin half-cells were cycled with the given electrolytes using a TOSCAT-3100 charge/discharge machine (Toyo System, Iwaki, Japan). The graphite|Li coin half-cells were charged (lithiated) in a consecutive two-step constant-current (0.5C)/constant-potential (0.01 V until 0.05C) process. Discharging (delithiation) was performed at a constant current of 0.5C up to 1.5 V. The $LiFePO_4$|Li coin half-cells were cycled in the potential range of 3.7–3.0 V at a slow constant current of 0.1C or 0.3C. The C-rate was calculated based on the theoretical capacities of the active materials (graphite: 372 mAh g^{-1} and

$LiFePO_4$: 170 mAh g^{-1}). Cyclic voltammetry was conducted with $LiFePO_4$|Li coin half-cells in DMAP-based electrolytes at a scanning rate of 0.05 mV s^{-1}.

The interfacial resistance of fully charged graphite anodes was evaluated via electrochemical impedance spectroscopy (EIS) with an amplitude of 10 mV over the frequency range 10 mHz–1 MHz. The LSV curves of graphite|Li coin half-cells in 1 M LiFSI/DMAP:FEMC electrolytes were obtained at a scanning rate of 0.1 mV s^{-1}. The oxidation stabilities of the electrolytes were estimated via LSV with a Pt|Li|Li three-electrode cell from the open-circuit potential up to 6 V (vs. Li/Li^+) at a slow scanning rate of 0.1 mV s^{-1}. The Al|Li floating test was performed with Al current collectors as the working electrodes and Li metal as the counter and reference electrodes from the open-circuit voltage (OCV; 3.6 V) to 6.0 V. All of above tests (EIS, LSV, and floating test) were conducted using VMP3 potentiostat (BioLogic, Seyssinet-Pariset, France).

Characterizations: The viscosity of the prepared electrolytes was measured using an EMS-1000S viscometer (Kyoto Electronics Manufacturing, Kyoto, Japan). The ionic conductivity was determined by measuring the alternating current impedance spectrum using a Pt|electrolyte|Pt cell over the frequency range from 100 mHz to 10 kHz. The density of DMAP solvent was measured at 60 °C by an Anton Paar density meter (Anton Paar GmbH, Austria). The basic physicochemical properties of the DMAP solvent and DMAP-based electrolytes are summarized in **Table S1**.

TEM observation and EDS analysis were conducted using JEM-ARM200F (JEOL, Japan) and JED-2300 (EX-24280M1G5T, JEOL, Japan). A cross-section of electrode samples was prepared with a focused ion beam (SMF2000, Hitachi High-tech, Japan) and transferred into the TEM chamber without air exposure.

The water contents of the solvent and electrolyte were estimated using a Karl Fischer coulometric titrator (CA-21, Mitsubishi Chemical Analytech, Yamato, Japan).

DSC was performed using a C-600 (Setaram, Cranbury, NJ, USA) to evaluate the exothermic behaviors of fully lithiated graphite in various electrolytes. Graphite|Li coin half-cells, which were fabricated with the given electrolytes, were cycled once in the potential range of 0.01–1.5 V and charged again in a consecutive two-step constant-current (0.5C)/constant-potential (0.01 V until 0.05C) process. After disassembling the cell, the electrode was washed several times with DMC in an Ar-filled glovebox. The fully lithiated graphite powder collected from the electrode (25 mg) and fresh electrolyte (15 mg) were placed in a specially designed pressure-resistant container and tightly sealed with a 25 Nm torque wrench. The container was stabilized at 50 °C for 2 h and then heated to 300 °C at 0.5 °C min^{-1}. An empty container was used as a reference, and the instrumental baseline was corrected by subtracting the blank curve from the raw data.

Declaration of interests

The authors declare no competing interests.

Data availability

Data relating to the materials, methods, experimental procedures, and other characterizations are available in the supplemental information.

Supporting Information

The Supporting Information is available free of charge at

A detailed description of the physicochemical and electrochemical properties of the newly synthesized 2-(N,N-dimethylamino)-1,3,2-dioxaphospholane 2-oxide (DMAP) solvent and DMAP-based electrolytes; ^{1}H-NMR, ^{13}C-NMR, and ^{31}P-NMR analyses; flammability tests; moisture stability assessments; comparison of cycling stability and CE of graphite|Li and $LiFePO_4$|Li cells; LSV curves, EIS results, and rate performance of graphite|Li cells; XPS and TEM analysis of the SEI on the graphite anode; DSC thermograms and overall heat generation of fully lithiated graphite anode; electrolyte oxidation stability; CV curves of $LiFePO_4$|Li cells; chronoamperometry (floating test) profiles of Al|Li cells; and XPS spectra of passivated Al electrodes.

Acknowledgements

This work was supported by a Japan Society for the Promotion of Science Grant-in-Aid for Scientific Research (S, Grant Number 20H05673) and the Japan Science and Technology Agency Program on Open Innovation Platform for Industry-Academia Co-Creation (Grant Number JPMJPF2016).

References

(1) Li, M.; Lu, J.; Chen, Z.; Amine, K. 30 Years of Lithium-Ion Batteries. *Adv Mater* **2018**, *30* (33), 1800561.

(2) Zeng, X.; Li, M.; Abd El-Hady, D.; Alshitari, W.; Al-Bogami, A. S.; Lu, J.; Amine, K. Commercialization of Lithium Battery Technologies for Electric Vehicles. *Adv Energy Mater* **2019**, *9* (27), 1900161.

(3) Zubi, G.; Dufo-López, R.; Carvalho, M.; Pasaoglu, G. The Lithium-Ion Battery: State of the Art and Future Perspectives. *Renew Sustain Energy Rev* **2018**, *89*, 292–308.

(4) Diouf, B.; Pode, R. Potential of Lithium-Ion Batteries in Renewable Energy. *Renew Energy* **2015**, *76*, 375–380.

(5) Chen, Y.; Kang, Y.; Zhao, Y.; Wang, L.; Liu, J.; Li, Y.; Liang, Z.; He, X.; Li, X.; Tavajohi, N.; Li, B. A Review of Lithium-Ion Battery Safety Concerns: The Issues, Strategies, and Testing Standards. *J Energy Chem* **2021**, *59*, 83–99.

(6) Wang, Y.; Feng, X.; Huang, W.; He, X.; Wang, L.; Ouyang, M. Challenges and Opportunities to Mitigate the Catastrophic Thermal Runaway of High-Energy Batteries. *Adv Energy Mater* **2023**, *13* (15), 2203841.

(7) Liu, X.; Yin, L.; Ren, D.; Wang, L.; Ren, Y.; Xu, W.; Lapidus, S.; Wang, H.; He, X.; Chen, Z.; Xu, G.-L.; Ouyang, M.; Amine, K. In Situ Observation of Thermal-Driven Degradation and Safety Concerns of Lithiated Graphite Anode. *Nat Commun* **2021**, *12* (1), 4235.

(8) Yang, H.; Bang, H.; Amine, K.; Prakash, J. Investigations of the Exothermic Reactions of Natural Graphite Anode for Li-Ion Batteries during Thermal Runaway. *J Electrochem Soc* **2005**, *152* (1), A73.

(9) Zu, C.; Yu, H.; Li, H. Enabling the Thermal Stability of Solid Electrolyte Interphase in Li-ion Battery. *InfoMat* **2021**, *3* (6), 648–661.

(10) Peled, E.; Menkin, S. Review—SEI: Past, Present and Future. *J Electrochem Soc* **2017**, *164* (7), A1703–A1719.

(11) Agubra, V. A.; Fergus, J. W. The Formation and Stability of the Solid Electrolyte Interface on the Graphite Anode. *J Power Sources* **2014**, *268*, 153–162.

(12) Andersson, A. M.; Herstedt, M.; Bishop, A. G.; Edström, K. The Influence of Lithium Salt on the Interfacial Reactions Controlling the Thermal Stability of Graphite Anodes. *Electrochim Acta* **2002**, *47* (12), 1885–1898.

(13) Ryou, M.-H.; Lee, J.-N.; Lee, D. J.; Kim, W.-K.; Jeong, Y. K.; Choi, J. W.; Park, J.-K.; Lee, Y. M. Effects of Lithium Salts on Thermal Stabilities of Lithium Alkyl Carbonates in SEI Layer. *Electrochim Acta* **2012**, *83*, 259–263.

(14) Hou, J.; Lu, L.; Wang, L.; Ohma, A.; Ren, D.; Feng, X.; Li, Y.; Li, Y.; Ootani, I.; Han, X.; Ren, W.; He, X.; Nitta, Y.; Ouyang, M. Thermal Runaway of Lithium-Ion Batteries Employing $LiN(SO_2F)_2$-Based Concentrated Electrolytes. *Nat Commun* **2020**, *11* (1), 5100.

(15) Aspern, N.; Leissing, M.; Wölke, C.; Diddens, D.; Kobayashi, T.; Börner, M.; Stubbmann-Kazakova, O.; Kozel, V.; Röschenthaler, G.; Smiatek, J.; Nowak, S.; Winter, M.; Cekic-Laskovic, I. Non-Flammable Fluorinated Phosphorus(III)-Based Electrolytes for Advanced Lithium-Ion Battery Performance. *ChemElectroChem* **2020**, *7* (6), 1499–1508.

(16) Han, J.; Kim, K.; Lee, Y.; Choi, N. Scavenging Materials to Stabilize $LiPF_6$-Containing Carbonate-Based Electrolytes for Li-Ion Batteries. *Adv Mater* **2019**, *31* (20), 1804822.
(17) Shi, P.; Zheng, H.; Liang, X.; Sun, Y.; Cheng, S.; Chen, C.; Xiang, H. A Highly Concentrated Phosphate-Based Electrolyte for High-Safety Rechargeable Lithium Batteries. *Chem Commun* **2018**, 54, 4453-4456.
(18) Wang, J.; Yamada, Y.; Sodeyama, K.; Watanabe, E.; Takada, K.; Tateyama, Y.; Yamada, A. Fire-Extinguishing Organic Electrolytes for Safe Batteries. *Nat Energy* **2018**, *3* (1), 22–29.
(19) Zeng, Z.; Murugesan, V.; Han, K. S.; Jiang, X.; Cao, Y.; Xiao, L.; Ai, X.; Yang, H.; Zhang, J.-G.; Sushko, M. L.; Liu, J. Non-Flammable Electrolytes with High Salt-to-Solvent Ratios for Li-Ion and Li-Metal Batteries. *Nat Energy* **2018**, *3* (8), 674–681.
(20) Wang, X.; Yasukawa, E.; Kasuya, S. Nonflammable Trimethyl Phosphate Solvent-Containing Electrolytes for Lithium-Ion Batteries: I. Fundamental Properties. *J Electrochem Soc* **2001**, *148* (10), A1058.
(21) Fan, X.; Chen, L.; Borodin, O.; Ji, X.; Chen, J.; Hou, S.; Deng, T.; Zheng, J.; Yang, C.; Liou, S.-C.; Amine, K.; Xu, K.; Wang, C. Non-Flammable Electrolyte Enables Li-Metal Batteries with Aggressive Cathode Chemistries. *Nat Nanotechnol* **2018**, *13* (8), 715–722.
(22) An, K.; Tran, Y. H. T.; Kwak, S.; Han, J.; Song, S. Design of Fire-Resistant Liquid Electrolyte Formulation for Safe and Long-Cycled Lithium-Ion Batteries. *Adv Funct Mater* **2021**, *31* (48), 2106102.
(23) Zheng, Q.; Yamada, Y.; Shang, R.; Ko, S.; Lee, Y. Y.; Kim, K.; Nakamura, E.; Yamada, A. A Cyclic Phosphate-Based Battery Electrolyte for High Voltage and Safe Operation. *Nat Energy* **2020**, *5* (4), 291–298.
(24) Su, C.-C.; He, M.; Peebles, C.; Zeng, L.; Tornheim, A.; Liao, C.; Zhang, L.; Wang, J.; Wang, Y.; Zhang, Z. Functionality Selection Principle for High Voltage Lithium-Ion Battery Electrolyte Additives. *ACS Appl Mater Interfaces* **2017**, *9* (36), 30686–30695.
(25) Zhang, S.; Li, A.; Zou, J.; Lin, L. Y.; Wooley, K. L. Facile Synthesis of Clickable, Water-Soluble, and Degradable Polyphosphoesters. *ACS Macro Lett* **2012**, *1* (2), 328–333.
(26) Lai, J.; Huang, Y.; Zeng, X.; Zhou, T.; Peng, Z.; Li, Z.; Zhang, X.; Ding, K.; Xu, C.; Ying, Y.; Cai, Y.-P.; Shang, R.; Zhao, J.; Zheng, Q. Molecular Design of Asymmetric Cyclophosphamide as Electrolyte Additive for High-Voltage Lithium-Ion Batteries. *ACS Energy Lett* **2023**, *8* (5), 2241–2251.
(27) Alpen, U. v. Li_3N: A Promising Li Ionic Conductor. *J Solid State Chem* **1979**, *29* (3), 379–392.
(28) Kawasoko, H.; Shiraki, S.; Suzuki, T.; Shimizu, R.; Hitosugi, T. Extremely Low Resistance of Li_3PO_4 Electrolyte/$Li(Ni_{0.5}Mn_{1.5})O_4$ Electrode Interfaces. *ACS Appl Mater Interfaces* **2018**, *10* (32), 27498–27502.
(29) Wang, Y.; Zhang, Q.; Xue, Z.; Yang, L.; Wang, J.; Meng, F.; Li, Q.; Pan, H.; Zhang, J.; Jiang, Z.; Yang, W.; Yu, X.; Gu, L.; Li, H. An In Situ Formed Surface Coating Layer Enabling $LiCoO_2$ with Stable 4.6 V High-Voltage Cycle Performances. *Adv Energy Mater* **2020**, *10* (28), 2001413.
(30) Lee, S.-W.; Kim, M.-S.; Jeong, J. H.; Kim, D.-H.; Chung, K. Y.; Roh, K. C.; Kim, K.-B. Li_3PO_4 Surface Coating on Ni-Rich $LiNi_{0.6}Co_{0.2}Mn_{0.2}O_2$ by a Citric Acid Assisted Sol-

Gel Method: Improved Thermal Stability and High-Voltage Performance. *J Power Sources* **2017**, *360*, 206–214.

(31) Shukor, F.; Hassan, A.; Saiful Islam, Md.; Mokhtar, M.; Hasan, M. Effect of Ammonium Polyphosphate on Flame Retardancy, Thermal Stability and Mechanical Properties of Alkali Treated Kenaf Fiber Filled PLA Biocomposites. *Materials & Design* **2014**, *54*, 425–429.

(32) Hämäläinen, J.; Holopainen, J.; Munnik, F.; Hatanpää, T.; Heikkilä, M.; Ritala, M.; Leskelä, M. Lithium Phosphate Thin Films Grown by Atomic Layer Deposition. *J Electrochem Soc* **2012**, *159* (3), A259–A263.

(33) Guo, K.; Qi, S.; Wang, H.; Huang, J.; Wu, M.; Yang, Y.; Li, X.; Ren, Y.; Ma, J. High-Voltage Electrolyte Chemistry for Lithium Batteries. *Small Science* **2022**, *2* (5), 2100107.

(34) Wang, Z.; Sun, Z.; Shi, Y.; Qi, F.; Gao, X.; Yang, H.; Cheng, H.; Li, F. Ion-Dipole Chemistry Drives Rapid Evolution of Li Ions Solvation Sheath in Low-Temperature Li Batteries. *Adv Energy Mater* **2021**, *11* (28), 2100935.

(35) Zhang, Z.; Hu, L.; Wu, H.; Weng, W.; Koh, M.; Redfern, P. C.; Curtiss, L. A.; Amine, K. Fluorinated Electrolytes for 5 v Lithium-Ion Battery Chemistry. *Energy Environ Sci* **2013**, *6* (6), 1806–1810.

(36) Padhi, A. K.; Nanjundaswamy, K. S.; Goodenough, J. B. Phospho-olivines as Positive-Electrode Materials for Rechargeable Lithium Batteries. *J Electrochem Soc* **1997**, *144* (4), 1188–1194.

(37) Yamada, A.; Chung, S. C.; Hinokuma, K. Optimized $LiFePO_4$ for Lithium Battery Cathodes. *J Electrochem Soc* **2001**, *148* (3), A224.

(38) Zhao, L.; Sun, Z.; Zhang, H.; Li, Y.; Mo, Y.; Yu, F.; Chen, Y. An Environment-Friendly Crosslinked Binder Endowing $LiFePO_4$ Electrode with Structural Integrity and Long Cycle Life Performance. *RSC Adv* **2020**, *10* (49), 29362–29372.

(39) Yu, Z.; Rudnicki, P. E.; Zhang, Z.; Huang, Z.; Celik, H.; Oyakhire, S. T.; Chen, Y.; Kong, X.; Kim, S. C.; Xiao, X.; Wang, H.; Zheng, Y.; Kamat, G. A.; Kim, M. S.; Bent, S. F.; Qin, J.; Cui, Y.; Bao, Z. Rational Solvent Molecule Tuning for High-Performance Lithium Metal Battery Electrolytes. *Nat Energy* **2022**, *7* (1), 94–106.

(40) Aurbach, D.; Markovsky, B.; Salitra, G.; Markevich, E.; Talyossef, Y.; Koltypin, M.; Nazar, L.; Ellis, B.; Kovacheva, D. Review on Electrode–Electrolyte Solution Interactions, Related to Cathode Materials for Li-Ion Batteries. *J Power Sources* **2007**, *165* (2), 491–499.

(41) Byeon, P.; Bae, H. Bin; Chung, H.-S.; Lee, S.-G.; Kim, J.-G.; Lee, H. J.; Choi, J. W.; Chung, S.-Y. Atomic-Scale Observation of $LiFePO_4$ and $LiCoO_2$ Dissolution Behavior in Aqueous Solutions. *Adv Funct Mater* **2018**, *28* (45), 1804564.